DIGITAL TERRAIN MODELS AND THEIR USABILITY TO LANDSLIDE RISK ASSESSMENT AND VISUALISATION

Manuela Hirschmugl[1], Klaus Granica[1], Herwig Proske[1], Michael Wurm[1], Alexander Almer[1], Thomas Schnabel[1], Johann Raggam[1], Mathias Schardt[1]

1. JOANNEUM RESEARCH, Institute of Digital Image Processing, Graz, Austria; manuela.hirschmugl@joanneum.at

ABSTRACT

Digital Terrain Models (DTMs) are an important information source for many remote sensing and GIS applications. In this paper, the usability of DTMs from different sources for the mapping of landslide susceptibility as well as for visualisation purposes is evaluated. The work was done within the scope of the ASSIST (Alpine Safety, Security & Informational Services and Technologies) project and results were exchanged over the GMOSS (Global Monitoring for Security and Stability) Network of Excellence. An Alpine testsite has been selected in a high mountain terrain near Landeck/Tyrol (Austria). This region is prone to many natural hazards, i.e. landslides, floods and snow avalanches. A DTM with a spatial resolution of 25 m and a very high resolution LiDAR DTM offering a spatial resolution of 2 m were used to identify geomorphometric parameters as indicators for landslide susceptibility mapping. Additionally to these indicators, also landcover information from a QUICKBIRD satellite image classification and geological data extracted from a geological map are used in this testsite. The differences between the two DTMs in the context of assessing risk zones based on statistical models are evaluated and compared to visual aerial image interpretation of risk zones. Additionally, a region in Kashmir was selected as a second testsite to evaluate the usability of a DTM derived from three SPOT5 scenes for the derivation of landslide indicators. Furthermore, an overview is given on the usability of the different DTMs for geo-visualisation.

1. INTRODUCTION

The detection of landslide susceptibility zones is a very labour-intensive work either performed in a field campaign or by applying visual interpretation on remote sensing data. Generally, the occurrence of mass movements is influenced by quasi-static factors such as the inclination of the slope or the land cover type and also by dynamic factors like rainfall. Quasi-static means, that these factors are normally stable over a period of time. In this study, the factors were divided into the following main categories: (a) geology; (b) geomorphology / topography; (c) land cover.

The triggering factors (dynamic factors) for an actual landslide event are temporal ones such as abundant rainfall, rapid spring snow melt or earthquakes. For the generation of the current susceptibility map, the triggering factors are not taken into account.

Due to time and cost restrictions, indicators for the quasi-static factors should be extracted as automatic as possible, but with sufficient detail. Geologic information can be obtained from geological maps integrated into a GIS environment. The use of a digital terrain model (DTM) is the main information source for the derivation of the required geomorphometric features. Very high resolution imagery (VHR), such as QUICKBIRD or IKONOS imagery, is one possible data source to derive the required land cover information as well as some additional information for the derivation of geomorphometric features.

Within the frame of landslide susceptibility mapping, the specific aims of this study are to:

→ Test different DTMs with respect to their usability to derive geomorphometric features

→ Evaluate the geomorphometric features regarding their use for susceptibility mapping

→ Assess the applicability of different DTMs for data visualisation

2. DATA

The basic geologic information was taken from a geological map at a scale of 1:50 000 (Austrian Geological Survey GBA); the land cover parameters were derived from a QUICKBIRD scene and the geomorphometric features were calculated based on DTMs from different sources. In the Austrian testsite, two data sets are directly compared: the standard DTM with 25 m resolution and a detailed LiDAR DTM with a resolution of 2 m. To evaluate also the applicability of the DTM from multi image stereo matching, an example from the Kashmir region is used. The details of the LiDAR data and the SPOT stereo data as the basis for the stereo DTM can be found in Table 1. The first data set to be tested is a DTM from the Austrian national land survey 'BEV'. This DTM shows a varying accuracy depending on the complexity of the terrain. The accuracy is stated to be about ± 2 – 5 m in non-forested and flat areas and ± 10 - 25 m in mountainous terrain or beneath forest (according to (i)). Since landslide activity is linked to a certain inclination and as large parts of the testsite area are covered with forest, the lower accuracy values are more reasonable for the current study. The second available DTM was derived from LiDAR (Light Detection And Ranging) data. The general accuracy of LiDAR DTMs depends on the used point density and on the vegetation cover. LiDAR systems offer good terrain information also beneath forest.

Table 1: Technical specification of the remote sensing input data (SPOT stereo imagery for Kashmir and LiDAR data for Austria).

Parameter	**SPOT PANCHROMATIC triplet**			**Parameter**	**LiDAR Optech**
Acquisition date	**6.10.2004**	**21.10.2005**	**18.12.2005**	**Acquisition date**	**2006**
Orbit	**197/281**			**Flying height**	**Approx. 1800 m**
Spatial resolution	**Panchromatic: 2.5 m**			**Point density**	**On average: 1.1/m²**
Spectral resolution	**Panchromatic: 0.61 – 0.68 µm**			**Overlap**	**30%**
Look angle	**+11.4**	**-1.8**	**-28.7**	**Field of View**	**±13°**

3. METHODS

This chapter is subdivided into three sections according to the corresponding aims. The first section deals with the derivation of DTMs from the data described above. In the second, the methods for the derivation of geomorphometric parameters from these generated DTMs are explained. Finally, the third section describes the two univariate statistical models used for susceptibility mapping. For these models, additional inputs, such as geological information, are necessary. In order to integrate this information into the landslide susceptibility modeling, the geological units from the available map were merged from the original 116 classes to 16 classes standing for distinct properties with respect to landslide occurrence. Furthermore, land cover information is important which was derived from orthorectified, topographically normalized and pansharpened QUICKBIRD imagery. A comparison between air photos and satellite imagery for susceptibility mapping can be found in Weirich & Blesius 2006 (ii). The land cover classification encompasses a hierarchical approach starting with a supervised pixel-wise classification using training areas and a maximum likelihood classifier. Subsequently, too small clusters were merged with the neighbouring classes and inherent texture information was used to distinguish spectrally similar classes like coarse and fine detritus. More details on the classification procedure can be found in Granica et al. 2007 (iii).

3.1 Obtaining DTMs

The BEV DTM has been derived by a combination of photogrammetric measurements from airborne imagery and structure information such as ridges and breaklines. The resulting information was then interpolated to a regular raster of 25 m. Details can be found in BEV 2007().

The LiDAR DTM was calculated from the original point cloud by a filtering approach called 'gridbased hierarchical weighting function approach' described in Wack & Wimmer 2002 (**iv**). The

aim of the filter is to eliminate buildings and vegetation, leaving only the terrain structures at a resolution of 2 m.

A digital surface model (DSM) from three SPOT5 images was generated for the Kashmir testsite based on methods described in Raggam et al. 2007 (**v**). In non-vegetated areas, such a surface model is equivalent to a digital terrain model and can, therefore, be used as such. Due to very poor reference data (maps), the DTM from the first matching resulted in poor accuracy of about 60 m. Using the coarse existing SRTM (shuttle radar topography mission) DTM, the panchromatic images could be roughly orthorectified. With these roughly orthorectified images, the matching was performed again and the DTM could be improved to an absolute height accuracy of about 20 m. Since the aim in this study is not to evaluate the absolute accuracy but the usability for landslide modeling, relative consistency and details are more important than absolute height precision.

3.2 Deriving geomorphometric features

The geomorphologic situation can be seen as one of the most important factors for landslide processes. At the same time, the details are difficult to be assessed by means of automatic image processing tools. The spatial resolution of the used DTM has to be considered, if geomorphometric features like roughness parameters are derived. There are a few different approaches to automatically derive geomorphologic information:

1. Curvature: Curvature is basically the change of slope in any direction. It can roughly be divided into concave, convex and not curved.

2. Downslope curvature: This measure describes the curvature in the direction of the slope. In many cases, downslope facing – convex - forms indicate an enhanced potential for landsliding.

3. Eigenvectors (according to McKean 2004 (**vi**)) measure the variability of slope and aspect in local patches of the DTM. Unit vectors are constructed perpendicular to each cell in the DTM. On this basis, different statistical measures are applied to evaluate the local variability.

4. Hydrological stream net: A DTM can be used to calculate a theoretical hydrological stream net. More details in the DTM lead to a more realistic location of ditches and creeks. The distance to trenches can serve as an indicator for landslide susceptibility.

3.3 Modeling

According to Hansen 1984 (**vii**) there are two different approaches for hazard zone mapping: (a) direct approaches, also called hazard mapping, mainly based on field work and (b) indirect methods. The latter calculate the importance of the combinations of parameters, namely the pre-disposition, occurring in landslide locations and extrapolate the results to landslide-free areas with similar combinations, mainly by statistical models (Van Westen 1993 (**viii**)). In this study, both approaches were used. The first approach was used to derive the training and verification data. This was performed by on-screen interpretation of a simulated QUICKBIRD ‘pseudo-stereo’ image and field work. The second approach was used for the susceptibility analysis per se. Van Westen 2006 (**ix**) stated, that the triggering of different types of landslides (e.g. deep-seated rotational slides, shallow translational slides) depends on different parameter combinations. Therefore, different training data sets would be necessary for different types of landslides. Since shallow translational slides are predominant in the study area, the current investigation is solely restricted to this type. Two different statistical models were used to assess the susceptibility:

1. Weights of evidence (WoE) model:
   This method was developed by Bonham-Carter et al. 1988 (**x**) for gold exploration in Nova Scotia. Positive and negative weights are assigned to each factor (binary map) using Bayes’ theorem for conditional probability. According to Van Westen 1993 (viii), the final product is “a predictor map giving the posterior probability of the occurrence of landslides for each pixel, which is based upon the unique overlap of all binary input pattern maps”.
2. Susceptibility model:
   This method (implemented according to the description in Van Westen 1993 ( )) also belongs to the group of univariate statistical landslide hazard analysis methods.

The main differences between the two methods are that for the susceptibility model: (a) no negative weights are derived and (b) the weights are not logarithmised.

4. RESULTS

Quality of the land cover classification

The quality of the land cover classification based on QUICKBIRD imagery was assessed by using an independent test area set of 5 - 6 test areas for each class. The accuracies of each class are given in Table 2, the overall average accuracy is 89.67%. This accuracy is sufficient for the envisaged purpose.

Table 2: Accuracy values for the final land cover classification.

Classified as ➡ / Ground truth ⬇	0: shadow	1	2	3	4	5	6	7	8	9	10	11
1: rock	0,2	**67,6**	13,3	2,2	16,7	-	-	-	-	-	-	-
2: debris coarse	-	-	**83,1**	4,6	12,3	-	-	-	-	-	-	-
3: debris fine	-	3,0	3,0	**88,4**	5,6	-	-	-	-	-	-	-
4 non-vegetated	-	-	-	-	**99,9**	0,1	-	-	-	-	-	-
5 sparsely vegetated	-	-	-	-	1,4	**92,2**	-	-	-	6,4	-	-
6: Rhododendron	-	-	-	-	-	0,1	**97,7**	0,1	-	1,8	0,3	-
7: forest	-	-	-	-	-	0,2	-	**99,4**	-	0,4	-	-
8: intensive meadow	-	-	-	-	-	0,4	-	0,9	**90,7**	6,9	1,1	-
9: meagre or harvested meadow	-	-	-	-	0,1	3,4	-	0,3	-	**96,2**	-	-
10: Alpine meadow	-	-	-	-	-	0,3	4,7	-	-	8,8	**86,2**	-
11: buildings	-	-	-	-	0,1	5,1	-	9,3	-	0,5	-	**85,0**

Quality of the derived DTMs

Subsets of the resulting three DTMs (about 1400 m x 900 m) are shown in Figure 1 to demonstrate the quality of the models. BEV DTM and LiDAR DTM are displaying the same area and can therefore be directly compared. Clearly, the LiDAR DTM shows the best result with many details such as roads, creeks, ravines, etc. The SPOT stereo DTM from Kashmir also offers some details, while the BEV DTM is more generalized. The main weakness of the SPOT stereo DTM is the absence of terrain data over areas with dense and high vegetation such as forested areas. However, for areas covered by low vegetation or for bare ground, such a model is an option if no adequate basic DTM is available and a LiDAR campaign is too costly.

(a) BEV DTM *(b) LiDAR DTM* *(c) SPOT4 stereo DTM*

Figure 1: Visual comparison of the DTMs (subsets of ~1400 m x 900 m): (a) and (b) in Austria; (c) in Kashmir.

Results of the susceptibility modeling

The model was implemented and executed within an ArcGIS environment and comparisons between the susceptibility analysis and the WoE method were accomplished. Altogether 44 input classes were used for the analysis, of which more than a third consisted of geological classes. The

comparison of the results from the two models shows the different weighting of the input parameters, especially for geological inputs. Figure 2 focuses on a subset in the northern, carbonatic part of the study area. The result of the susceptibility method (left image) shows that the geological formation “cretaceous shales” has an unbalanced strong influence on the calculation. For instance, the homogeneously red colored patches in the centre of the left image clearly demonstrate this effect. On the other hand, the WoE method generally shows similar tendencies, but the areas are more structured, which gives a more realistic impression of the susceptible terrain.

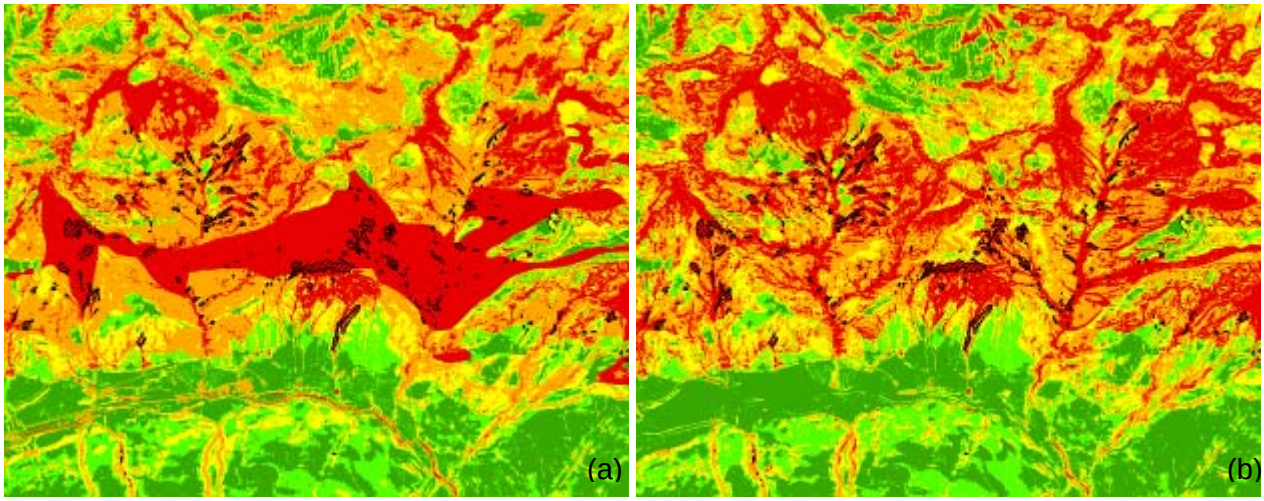

Figure 2: Subset (~7300 m x 5700 m) of the results of the susceptibility (a) and the weights of evidence method (b) of the study area. Colours indicate susceptibility class (green: lowest, red: highest) and hatched areas show the training landslides.

The colours are representing the continuous values for each pixel stretched from minimum to maximum in each of the subsets in Figure 2. It can clearly be seen that the WoE method is more selective and therefore better suitable. In order to transfer these continuous values into classes and to compare the results statistically, the values are classified into 5 classes. The classification scheme is based on deciles. Deciles 1 – 3 are assigned to the lowest susceptibility class (D1-3 → 1), the next three classes consist of 2 deciles each (D4+5 → 2; D6+7 → 3; D8+9 → 4). The 10th decile is equivalent to the highest susceptibility class (D10 → 5). This scheme has already proven to be useful in a former study (Proske et al., 2003; **xi**).

In order to evaluate the quality and transferability of the model (including the parameters), the testsite was divided into a western and an eastern part. The western area functioned as model-development area where the weights were calculated. These weights were then applied to the eastern part resulting in a susceptibility map of five classes according to the classification scheme described above. The results are evaluated by using the landslide inventory of the eastern part. The percentage of each landslide assigned to the five classes is calculated and the results from the western and eastern part are compared. This comparison is shown in Table 3. In the model-development area (west), the percentage in the highest risk class is almost 70%. On the contrary, in the model-evaluation area (east), only about 30% of the landslides were assigned to the highest class. However, the two highest ranked classes share, in both the model-development and the evaluation area, more than 75% of the landslide areas. Therefore, the method using the same weights can not be unrestrictedly transferred from one area to another.

Table 3: Transferability of the weights of evidence model parameters and -method.

Susceptibility class	1 (low)	2	3	4	5 (high)
East [%]	3,1	5,6	14,4	46,1	30,8
West [%]	1,5	1,9	6,4	20,8	69,4

4.2 Usability of different DTMs for susceptibility modeling

For the Austrian testsite, the susceptibility modeling with the two models including all derived parameters (land cover, geology, geomorphometric features) was performed and the differences of the resulting maps were analysed. For the Kashmir testsite, only the geomorphometric parameters were calculated and their results compared visually to those of the Austrian testsite.

It is important to mention, that during the susceptibility analysis, the parameter *aspect* turned out to be strongly biased and had to be excluded. The reason was found in the geologic situation of the testsite. The area is located at the border between carbonatic rock in the north (= south-facing slopes) and crystalline rock in the south (= north-facing slopes). Since landslides are much more frequent in the carbonate area, a high relevance is given to the parameter *aspect*, although the determinant factor of the landslide distribution is the specific geologic situation.

The general clusters remained the same for the calculation with the BEV DTM and the LiDAR DTM (see Figure 3). However, the model based on the LiDAR data shows a more pronounced result. Fine structures are better represented due to the differences in curvature and slope calculation. Based on the more detailed structure, the weights for the geomorphometric parameters also changed. However, there is no significant statistical difference between the LiDAR DTM based and the BEV DTM based susceptibility maps in the overall distribution of classes over the whole testsite. This effect is probably caused by two factors: (a) the coarse classes used for the calculation and (b) local differences which equalize over the whole area. In addition, the LiDAR data used in the current study has a point density of only 1.1 point per m². Further tests on LiDAR data with point densities around 4-6 dots per m² showed a higher potential than the lower resolution LiDAR DTM. Consequently, a resulting susceptibility map based on the high-point density LiDAR DTM shows more difference compared to the BEV DTM based map. However, this type of LiDAR data was not available for the whole testsite.

The SPOT stereo DTM, calculated from three images, is not as detailed as the LiDAR data. However, in remote areas high-resolution DTMs are hardly available, thus such a DTM can be used to compensate for this lack of data. The only alternative in remote regions is the SRTM DTM at a resolution of about 90 m. The curvatures calculated from the SPOT stereo DTM and the SRTM DTM were compared and are displayed in Figure 4. The spatial resolution clearly limits the capability of the SRTM DTM: only very rough features are visible. Data gaps occur in both models. Due to better geometric resolution, the SPOT stereo DTM was primarily used in the GMOSS project and only snow- or cloud-covered areas were filled with the SRTM DTM.

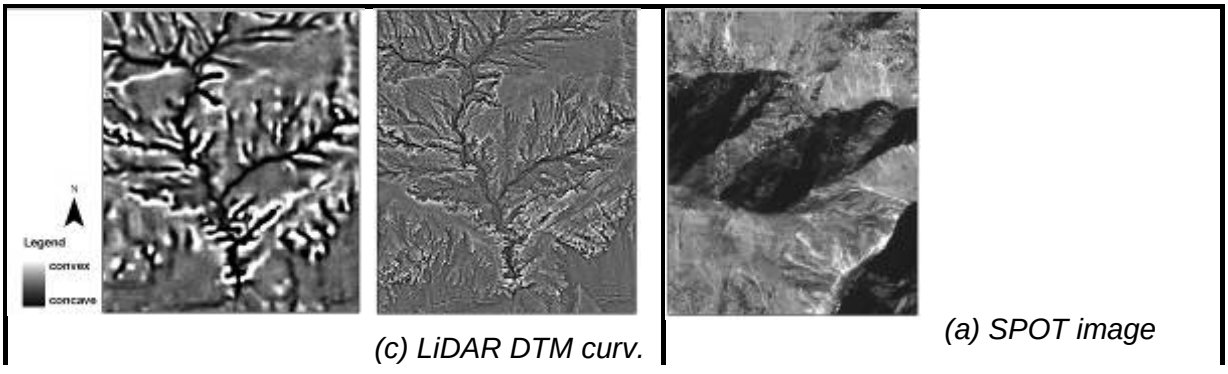

(c) LiDAR DTM curv. *(a) SPOT image*

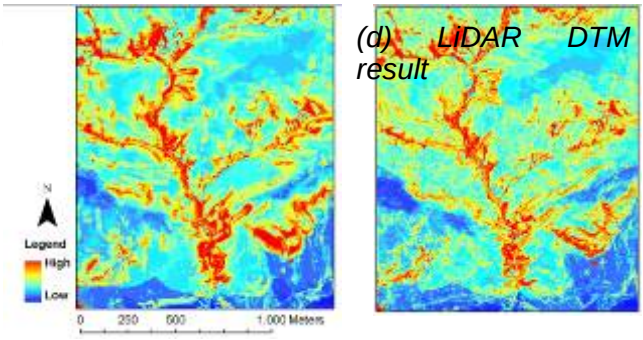

(d) LiDAR DTM result

Figure 3: Visual comparison of curvature calculation (above) and result of susceptibility analysis (below).

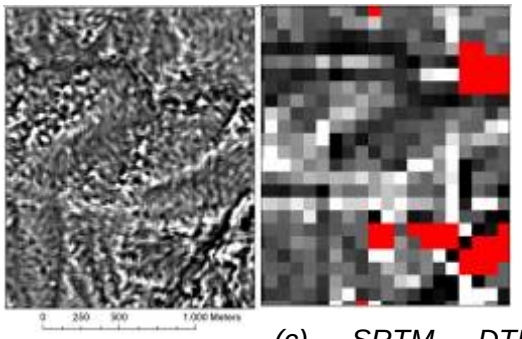

(b) SPOT DTM curv. *(c) SRTM DTM curv.*

Figure 4: Panchromatic SPOT image (a) and curvature calculated from the SPOT stereo DTM (b) and from the SRTM DTM (c). Red areas = missing data. Legend see Fig. 2 a.

4. 3. Usability of different DTMs for geo-visualisation

DTMs are of high importance as basic data for a 3D visualisation. Models using data from SRTM or BEV DTMs are only applicable for landscape visualisation at a lower resolution. For more detailed 3D models, high detailed DTMs derived from high resolution remote sensing stereo images or LiDAR data are the preferred choice. Additionally, the field of application is a crucial factor for the selection of a DTM. In the present project one had to differentiate between real-time and pre-processed modeling applications. For real-time applications, VHR DTMs are problematic due to their demands on a performance of high end graphic-cards, although VHR data gives the most realistic visual impressions. Depending on the purpose, there are many software products at hand to create these models, e.g. Visual Nature Studio, Maya, Java. Another option to use DTMs for geo-visualisation is by employing currently available OGC-Services. Examples for these are the Web Map Service (WMS), Web Terrain Server (WTS) and the Web 3D Service (W3DS). A WMS provides the data in a raster format in the requested resolution, dimension and format for another application (e.g. Shockwave 3D) that uses it as basic data for creating the model (WMS 2007; **xii**). The task of WTS is the building of perspective views of geo-referenced data. These exported views are in most cases formats like PNG, GIF or JPEG and not the data itself (WebTerrainServer 2007 (**xiii**)). W3DS is a portrayal service for three-dimensional geo-data, delivering graphical elements from a given geo-graphical area. In contrast to WMS and WTS, 3D scene graphs are produced. These scene graphs will be rendered by the client and can interactively be explored by the user. The W3DS merges different layers of 3D data in one scene graph (Web 3d Service 2007 (**xiv**)).

Recent projects have shown the importance of selecting the best suitable DTM for the visualisation depending on scale, application, costs and thematic requirements. VHR LiDAR DTMs proved to be best suitable for detailed 3D views including small geomorphologic structures and detailed vegetation, while the BEV DTM is sufficiently accurate for region-wide visualisations for tourism including e. g. hiking routes and 3D flights.

5. CONCLUSIONS

Landslide susceptibility analysis using univariate statistical models is a complex and sensitive task. The selection of appropriate input parameters and representative training data sets are crucial for the success of any model. The classification of QUICKBIRD data proved to deliver statistically accurate landcover classes, which have been used as variables in the susceptibility analysis. Additionally, a ‘pseudo-stereo’ image was generated from the QUICKBIRD satellite image and has

shown to be very useful for the visual interpretation of landslides in a time- and cost-saving manner. The different qualities of the used DTMs are clearly discernable in the final susceptibility maps. Although the difference in the overall statistics is only moderate, it is recommended to use a DTM with the finest resolution available, in order to pinpoint the hazardous spots in detail. For remote areas, often lacking detailed DTM data, the use of multi image matching procedures based on SPOT scenes is a possibility to obtain a DTM suitable for landslide susceptibility analysis, although it is only restricted to non vegetated areas. The applied statistical model for landslide susceptibility could not yet be evaluated in real situations, since no recent landslides within the study area have occurred. Up to now the only possible way for its evaluation was to focus on the approach encompassing a model-development and a model-evaluation area. This test showed that the model is not unrestrictedly transferable. For data visualisation the selection of the most appropriate DTM depends highly on the envisaged application, its aims and the level of thematic details.

REFERENCES

i BEV (Bundesamt für Eich- und Vermessungswesen), 2007. Produktinformation Digitales Geländehöhenmodell. Available at: http://www.austrianmap.at/bevportal/Produkte/pdf/dgm-hr.pdf [accessed May 2007].

ii Weirich, F. & Blesius, L., 2006. Comparison of Satellite and Air Photo Based Landslide Susceptibility Maps. Volume 87, Issue 4, pp. 352-364

iii Granica, K., Almer, A., Hirschmugl, M., Proske, H., Wurm, M., Schnabel, Th., Kenyi, L.W. & Schardt, M., 2007. Generation and webGIS representation of landslide susceptibility maps using VHR satellite data. To be published in: Proceedings of IGARSS2007, Barcelona, July, 23rd – 27th 2007.

iv Wack, R. & Wimmer, A., 2002. Digital Terrain Models from Airborne Laserscanner Data – a Grid based approach. Proceedings of the ISPRS Commission III Symposium Graz, pp. 293-296.

v Raggam, J., Wack, R. & Gutjahr, K.H., 2007. Mapping capability of a low-cost aerial data acquisition platform – first results. In Proceedings of ISPRS Hannover Workshop 2007, „High-Resolution Imaging for Geospatial Information", May 29 – June 1, 2007, published on CD-ROM.

vi McKean, J. & Roering, J., 2004. Objective landslide detection and surface morphology mapping using high-resolution airborne laser altimetry. Geomorphology 57 (2004), pp. 331-351.

vii Hansen, M. J., 1984. Strategies for classification of landslides. In: Slope Instability. D. Brunsden and D. B. Prior (Eds.), Wiley & Sons, New York, pp. 1-25.

viii Van Westen, C. J. 1993. Training package for geographic information systems in slope instability zonation. Vol. 1: Theory: Application of geographic information systems to landslide hazard zonation. ITC publication No. 15, International Institute for Aerospace Survey and Earth Sciences, Enschede, The Netherlands.

ix Van Westen, C.J., van Asch, T.W.J., Soeters, R., 2006. Landslide hazard and risk zonation – why is it still so difficult? Bull.Eng.Geol.Env. (2006) 65: 167-184.

x Bonham-Carter, G.F., Agterberg, F.P. & Wright, D.F. 1988. Integration of geological datasets for gold exploration in Nova Scotia: In Photogrammetric Engineering and Remote Sensing, v. 54(11), p. 1585-1592.

xi Proske et al. (2003): „PRERISK - Erarbeitung von Grundlagen für Prognose- und Vorwarnsysteme für das Risiko- und Katastrophenmanagement.", Endbericht JOANNEUM Research, Graz, Februar 2003, pp. 130.

xii WMS. 2007. http://portal.opengeospatial.org/files/?artifact_id=16075 [accessed: May 2007]

xiii WebTerrainServer. 2007. http://portal.opengeospatial.org/files/?artifact_id=1072 [accessed: May 2007]

xiv Web 3D Service. 2007. https://portal.opengeospatial.org/files/?artifact_id=8869 [accessed May 2007]